RESEARCH ARTICLE

Comparative evaluation of drought indices for monitoring drought based on remote sensing data

Wei Wei[1] · Jing Zhang[1] (ID) · Liang Zhou[2,3] · Binbin Xie[4] · Junju Zhou[1] · Chuanhua Li[1]

Abstract

Many indices are used to monitor drought events. However, different indices have different data requirements and applications. Hence, evaluating their applicability will help to characterize drought events and refine the development of effective drought indices. We constructed different drought indices based on multisource remote sensing data and comprehensively evaluated and compared their applicability for drought monitoring throughout China. The characteristics of drought events in 2009 and 2011 were compared using various drought indices. The different time scales of the Palmer Drought Severity Index (PDSI) and the Standardized Precipitation Index (SPI) were used to evaluate remote sensing drought indices in different regions. Single drought indices, including the Vegetation Condition Index (VCI), the Temperature Condition Index (TCI) derived from Moderate Resolution Imaging Spectroradiometer (MODIS) data, the Precipitation Condition Index (PCI) derived from Tropical Rainfall Measurement Mission (TRMM) data, and the TCI and Soil Moisture Condition Index (SMCI) derived from Advanced Microwave Scanning Radiometer for the Earth Observing System (AMSR-E) data, as well as combined drought indices, including the Microwave Integrated Drought Index (MIDI), Optimized Vegetation Drought Index (OVDI), Optimized Meteorological Drought Index (OMDI), Scale Drought Conditions Index (SDCI), and Synthesized Drought Index (SDI), were analyzed and compared to evaluate their applicability. The results showed that different drought indices have specific characteristics under different land use types in China. The VCI and TCI can better monitor long-term drought conditions, but they have a weak correlation with the in situ drought index in forestland and grassland areas. The correlation of SPI-1 with the PCI is higher than that with other single indices, which indicates that the PCI is a good short-term drought index. The SMCI has a better correlation with the short-term in situ drought index, but it is not conducive to drought monitoring in areas such as densely forested land and grassland. The correlations of the in situ drought index with the combined drought indices (the MIDI, OVDI, OMDI, SDCI, and SDI) are better than those with the single drought indices.

Keywords Remote sensing · Drought monitoring · Combined drought index · Comparative evaluation · China

✉ Jing Zhang
  18251907576@163.com

[1] College of Geography and Environmental Science, Northwest Normal University, Lanzhou 730070, Gansu, China

[2] Faculty of Geomatics, Lanzhou Jiaotong University, Lanzhou 730070, China

[3] Institute of Geographic Sciences and Natural Resources Research, CAS, Beijing 100101, China

[4] School of Urban Economics and Tourism Culture, Lanzhou City University, Lanzhou 730070, Gansu, China

Introduction

Drought is one of the most harmful natural disasters in the world (Hagman 1984; Huang et al. 2006). Frequent and prolonged periods of droughts result in not only considerable economic losses but also severe social and environmental problems (Halwatura et al. 2017; Trenberth et al. 2003). Drought is usually classified into four types: meteorological drought, agricultural drought, hydrological drought, and socioeconomic drought (Dracup et al. 1980; Orville 1990). Meteorological drought is caused by a lack of precipitation that leads to abnormal water shortages caused by an imbalance between precipitation and evaporation. Agricultural drought leads to a lack of water available for plant growth; consequently, due to the influences of various external factors, the water

absorption and consumption of plants become imbalanced. Hydrological drought refers to a deficient supply of surface water and groundwater. Finally, socioeconomic drought refers to the water supply being insufficient to meet the needs of economic interests; hence, the cause of socioeconomic drought is an imbalance between the supply and demand of water resources in both the natural system and the human socioeconomic system. With the increasing severity, periodicity, randomness, and regional nature of drought and the rising frequency and impacts of drought in recent decades, research on drought has become increasingly important worldwide (Hayes et al. 1999; McKee et al. 1993), particularly with regard to drought indices (Keyantash and Dracup 2004; Wilhelmi and Wilhite 2002). Given the above, the timely and accurate monitoring of drought conditions using various drought indices is essential.

Drought indices are established to monitor drought by integrating weather variables such as precipitation, evapotranspiration, and temperature (Hao and Singh 2015; Jiao et al. 2019a; Wang et al. 2012). Drought indices based on meteorological data derived from meteorological stations are particularly effectively at monitoring drought. For example, the Palmer Drought Severity Index (PDSI) (Palmer 1965), Standardized Precipitation Index (SPI) (McKee et al. 1993), and Standardized Precipitation Evapotranspiration Index (SPEI) (Vicente-Serrano et al. 2010) are widely used for monitoring meteorological drought. Among these indices, the SPI is the most widely used and accepted by the scientific community (Hayes et al. 1999; Park et al. 2017; Zhang and Jia 2013) and is often used to evaluate the precision of other indices because of the simplicity of its theory and calculation process (McKee et al. 1993; Park et al. 2017). The SPI can be calculated flexibly at different time scales (e.g., 1, 2, 3, 6, 9, 12, and 24 months) according to the user's needs for monitoring meteorological, agricultural, or hydrological drought (Guttman 1999). However, ground-based observation sites cannot offer data with continuous spatial coverage, limiting the ability to monitor the regional spatial pattern of drought conditions in detail, especially in areas with sparse weather stations or high spatial variability (Karnieli et al. 2010; Rhee et al. 2010).

Drought monitoring based on remote sensing data can overcome the abovementioned challenges involved in collecting ground observation data and can be used to continuously monitor the processes of and changes in drought across both time and space (Hao et al. 2015). Moreover, a drought index based on remote sensing data can capture spatial details, making it the most promising tool for regional-scale drought monitoring. Remote sensing technology makes it possible to monitor the soil moisture and vegetation status over a large area (Rhee et al. 2010; Wu et al. 2013; Zhang et al. 2017). Thus, with the development of remote sensing technology, numerous types of remote sensing data have been made

available and have become an important data source for large-scale drought monitoring (Rhee et al. 2010). Consequently, several remote sensing-based drought indices have been established in a variety of disciplines. In recent years, with rapid technological developments, satellite measurements of solar-induced chlorophyll fluorescence (SIF), the energy that is re-excited after the absorption of light by vegetation during photosynthesis, has become an effective method for the global monitoring of photosynthesis (Frankenberg et al. 2011; Guanter et al. 2014). SIF is directly related to the photosynthetic rate of vegetation and can quickly reflect the impact of water stress on vegetation growth (Jiao et al. 2019c; Meroni et al. 2009; Wang et al. 2016). Accordingly, many researchers have evaluated the ability of SIF to monitor and assess drought (Sun et al. 2015). In addition, on the basis of the Normalized Difference Vegetation Index (NDVI), Badgley et al. (2017, 2019) proposed the near-infrared reflectance of vegetation (NIRv), the value of which is equal to the product of the near-infrared ground reflectance and NDVI. To a certain extent, NIRv takes into account the proportions of the reflectance from vegetation and soil in a pixel. Systematic studies have found that NIRv is highly consistent with SIF, photosynthetically active radiation components, and gross primary productivity (GPP). Moreover, the vegetation optical depth (VOD) indicator is closely related to the vegetation moisture content (Owe et al. 2008; Song et al. 2019) and thus has been widely used in drought monitoring research (Jackson and Schmugge 1991; van Dijk et al. 2013), while the vapor pressure deficit (VPD) is closely related to the joint mechanism of plant photosynthesis and transpiration (Buckley 2019; Kimball 2016; Manderscheid et al. 2016). Kogan (1995) obtained the Vegetation Condition Index (VCI) by scaling the NDVI value from 0 to 1 and using the maximum and minimum NDVI values for each location. At the same time, Kogan (1995) established the Temperature Condition Index (TCI) through determining the weight of the NDVI in the same way. Zhang and Jia (2013) used remote sensing data from the Tropical Rainfall Measurement Mission (TRMM) and the Advanced Microwave Scanning Radiometer for the Earth Observing System (AMSR-E) to construct the Precipitation Condition Index (PCI) and Soil Moisture Condition Index (SMCI) and used these indices to monitor the drought conditions in northern China. Rhee et al. (2010) comprehensively used land surface temperature (LST), NDVI, and TRMM precipitation data to propose the Scale Drought Conditions Index (SDCI), which is suitable for both arid and humid regions through a weighted combination, and successfully monitored agricultural drought in North Carolina and South Carolina in the USA. Du et al. (2013) used LST, NDVI, and TRMM precipitation data to obtain the TCI, VCI, and PCI and the integrated PCI, TCI, and VCI by using principal component analysis (PCA) to construct the Synthesized Drought Index (SDI) and applied

them to drought monitoring in Shandong Province, China, where good drought monitoring results were obtained. Zhang and Jia (2013) used the empirical weighting method to combine the TCI, PCI, and SMCI to establish the Microwave Integrated Drought Index (MIDI) and monitor meteorological drought in northern China. Hao et al. (2015) introduced constrained optimization methods to combine the VCI, TCI, PCI, and SMCI into an Optimized Vegetation Drought Index (OVDI) and an Optimized Meteorological Drought Index (OMDI) and used these two indices to monitor agricultural drought in Southwest China; these indices, which are mainly calculated by remote sensing data or provided as products, have become the most important source of information for drought monitoring. Zhang et al. (2017) designed a Process-based Accumulated Drought Index (PADI) based on precipitation, soil moisture, and vegetation conditions and comprehensively considered drought development and crop phenology in an agricultural drought assessment. Jiao et al. (2019b) used a geographically weighted regression (GWR) model and PCA to synthesize the TCI, VCI, PCI, and SMCI and proposed the station-enabled Geographically Independent Integrated Drought Index (GIIDI_station). Liu et al. (2020) used multivariate linear regression methods (MCDI) to combine the TCI, VCI, PCI, and SMCI. Wei et al. (2020) used the PCI, VCI, and TCI to construct the Temperature Vegetation Precipitation Dryness Index (TVPDI) through the spatial distance method.

In recent decades, the international research community has displayed growing interest in the comparison of drought indices (Dubovyk et al. 2019; Seiler et al. 1998; Zhou et al. 2012). Since different data requirements are imposed on the establishment of different drought indices, different approaches for quantifying drought exhibit different characteristics, and different drought indices are suitable for different situations. Therefore, the comparative analysis of drought indices is very important for different regions. Many scholars have compared and analyzed the advantages and disadvantages of drought indices according to different perspectives, applications, and methods. Gitelson et al. (1998) studied the applicability of the VCI and TCI in Poland, and the results showed that the average error of the TCI was better than that of the VCI in terms of crop yield. Seiler et al. (1998) verified the TCI and VCI in drought-affected areas in Argentina and found that they were in good agreement with precipitation. Singh et al. (2003) used the TCI and VCI for drought monitoring in India and found that the VCI was not suitable for drought monitoring therein. Bayarjargal et al. (2006) compared the VCI, TCI, Standardized Vegetation Index (SVI), Normalized Difference Vegetation Index Anomaly (NDVIA), ratio of LST to NDVI (LST/NDVI), and Drought Severity Index (DSI) in Mongolia, and a comparative study was conducted in the region; the results showed that these different drought

indices have different characteristics and different accuracies. Bhuiyan et al. (2006) compared the SPI, VCI, and groundwater index of northern India and found that the VCI was related only to the meteorology and hydrology and thus provided better meteorological drought monitoring results. Quiring and Ganesh (2010) compared the VCI with the in situ meteorological drought index for 254 counties in Texas and found that counties in northwestern and southwestern Texas have more significant correlations than counties in the east and along the Gulf Coast. Shahabfar et al. (2012) used correlation analysis to compare four remote sensing indices and five water balance parameters to analyze the applicability of remote sensing indices in different climatic regions of Iran. Zhou et al. (2012) compared the VCI and TCI with the Percentage of Average Seasonal Greenness (PASG), Percentage of Precipitation Anomalies (PPA), and SPI percentages in the central eastern region of China. Dubovyk et al. (2019) used the 0.5° spatial resolution monthly standard meteorological index and 1 km Vegetation Health Index (VHI) products to analyze the consistency of these drought indices with the vegetation conditions in Kazakhstan derived from the Moderate Resolution Imaging Spectroradiometer (MODIS) Enhanced Vegetation Index (EVI). Pouya et al. (2020) compared the applicability of three different indicators of agricultural drought in Iran and showed that the Multivariate Standardized Precipitation Index (MSPI) can be used for monitoring agricultural drought.

In China, long-term and high-frequency droughts greatly affect food security and economic development (Yuan et al. 2015). In severe cases, these droughts may even cause famine and affect social stability, among other problems. According to the National Bureau of Statistics of China (NBSC 2009), a total of 26 provinces (autonomous regions and municipalities) in the country experienced drought problems in 2009, and the land area affected by crops reached $29,258.80 \times 10^3$ hm^2, of which the area affected by disasters and the area without a crop harvest reached $13,197.10 \times 10^3$ hm^2 and 326.88×10^3 hm^2, respectively; the annual amount of food loss reached 34.849×10^8 kg, and the economic crop loss amounted to 43.344×10^8 yuan with a direct economic loss of 120.659×10^8 yuan. In addition, during the drought disaster that occurred in 2011, approximately 60% of the area was affected by natural disasters (NBSC 2011). Because economic losses caused by drought account for 35% of the total losses from various natural disasters, the two drought disasters that impacted China in 2009 and 2011 were selected to investigate the spatial variations of numerous drought indices.

The purpose of this research is to study drought indices based on multisource remote sensing data. Accordingly, a variety of typical drought monitoring indices (VCI, TCI, PCI, SMCI, SDCI, SDI, MIDI, OVDI, and OMDI) were constructed based on multisource remote sensing data to study the drought situation in China. We studied the spatial distribution

patterns and evolutionary characteristics of typical drought events in China to obtain a better understanding of the regional differentiation of drought conditions throughout the country. We comprehensively evaluated the applicability of different indices to monitoring the drought environment in China and compared the characteristics of the different drought indices (Table 1).

Study area and data

Study area

The scope of this study covers the entire China. China spans 3°51′ N–53°34′ N in latitude and 73°29′ E–135°04′ E in longitude, covering an area of about 9.6×10^6 km^2 (Fig. 1a). China includes 34 provinces (cities, autonomous regions), and the main land use types include forestland (24%), grassland (31%), water area (3%), construction land (2%), cultivated land (19%), and unutilized land (21%) (He et al. 2017). Cultivated land is mainly distributed in the northeast and central part, forestland is mainly distributed in northeast and south China, grassland is mainly distributed in the Inner Mongolia and Qinghai-Tibet Plateau, and unutilized land is mainly distributed in the northwest. In recent years, China has experienced severe short-term (monthly to quarterly) droughts (Wang et al. 2011; Feng et al. 2014), which leads to the increased threat of arable land drought (Piao et al. 2010). In order to better control the drought situation in China, it is necessary to carry out drought monitoring research in China.

Data and processing

Remote sensing data

The Moderate Resolution Imaging Spectroradiometer (MODIS) is one of the most important sensors developed by the National Aeronautics and Space Administration (NASA) on the Terra and Aqua satellites. MODIS data products are updated in a timely manner. We downloaded two MODIS land products from 2002 to 2011 (http://search.earthdata.nasa.gov/search). Twenty-two tiles (h23v04, h23v05, h24v04, h24v05, h25v03, h25v04, h25v05, h25v06, h26v03, h26v04, h26v05, h26v06, h27v04, h27v05, h27v06, h28v05, h28v06, h28v07, h28v08, h29v06, h29v07, h29v08) were used to cover the study area. MOD11A2 daytime surface temperature (LST) product data, with a time resolution of 8 days and a spatial resolution of 1 km, were used. The maximum value method was used to synthesize the 8-day LST product into monthly data for calculating TCI. The NDVI data of MODD13A2 and MYD13A2 were used in this study, which have a time resolution of 16 days and a spatial resolution of 1 km. The

MOD13A2 product starts on the first day of each year, and the MYD13A2 product starts on the 9th day of each year. The NDVI data are preprocessed and then processed into monthly data using the maximum value synthesis method for calculating VCI. The coverage is the same as the LST data, with a total of 22 images.

The TRMM satellite was launched in November 1997, and since then, several algorithms have been developed to estimate rainfall (Iguchi et al. 2000). In this study, the monthly precipitation products of TRMM (3B43) from 2002 to 2011 were downloaded, with a spatial resolution of 0.25° × 0.25°, expressed in monthly precipitation (mm/h), and the storage format is HDF. The data coverage is between 50°S~50°N and 180°W~180°E. We used ENVI software and ArcGIS software to transform and project TRMM (3B43) products for PCI calculation. Since there are no data for the area north of 50°N in China, Climatic Research Unit (CRU) data were used for extrapolation (Wei et al. 2020). TRMM (3B43) data are from the NASA Data and Information Service Center (DISC) (http://mirador.gsfc.NASA.gov/).

The soil moisture (SM) and LST data were jointly developed by the Amsterdam Vrije University and NASA Goddard Space Flight Center (VUA-NASA) based on the descent pattern of the Aqua satellite (Njoku et al. 2003; Owe et al. 2008). The Land Parameter Refutation Model (LPRM) was proposed and launched in May 2002. The AMSR-E has two polarization modes: horizontal polarization and vertical polarization. There are 6 bands in the 6.9–89 GHz range and 12 channels in total (Kawanishi et al. 2003; Parkinson 2003), with a spatial resolution of 0.25° × 0.25°. AMSR-E L3A soil moisture data were obtained from an official inversion of 6.9 GHz and 10.7 GHz, which was used to calculate the SMCI. The inversion instructions and methods can be obtained free of charge from the NASA website (Bindlish et al. 2003). The LST data are the AMSR-E L3 data obtained from the 37 GHz vertical polarization brightness temperature and were used to calculate TCI_VUA. The VUA-NASA SM/LST dataset has been intensively validated in multiple regions (De Jeu et al. 2008; Draper et al. 2009; Parinussa et al. 2008). The VUA-NASA products are in good agreement with the in situ SM/LST measurement results and have a strong correspondence with temporal and spatial precipitation.

Climatic research unit data

The CRU high-resolution gridded dataset is one of the most widely used near-surface climate datasets in the world (Harris et al. 2014). The CRU dataset contains climate variables such as the average temperature, daily temperature range, precipitation, water vapor pressure, and cloud cover. In CRU_ts4.03, the time coverage of the data is 1901–2018, and the spatial resolution is 0.5° × 0.5°. This study used the monthly average precipitation data in the CRU_ts4.03 dataset to calculate

Table 1 Description of commonly used drought indices

Drought index	Creation time	Type	Data source	Method	Resolution	Reference
PDSI	1965	Meteorological drought	Precipitation, temperature, and soil moisture	Based on water balance model		(Palmer 1965)
SC-PDSI	2004	Meteorological drought	Precipitation, potential evapotranspiration, soil moisture, etc.	Improved PDSI spatial comparability		(Wells et al. 2004)
SPI	1993	Meteorological drought	Precipitation	Based on the historical precipitation occurrence probability distribution function		(McKee et al. 1993)
SPEI	2010	Meteorological drought	Potential evapotranspiration and precipitation	Based on the historical deficiency of precipitation (P-PET) occurrence probability		(Vicente-Serrano et al. 2010)
VCI	1995	Condition Index	MODIS NDVI	$(NDVI_i - NDVI_{min})/(NDVI_{max} - NDVI_{min})$	1 km	(Kogan 1995)
TCI	1997	Condition Index	MODIS LST	$(LST_{max} - LST_i)/(LST_{max} - LST_{min})$	1 km	(Kogan 1997)
SMCI	2010	Condition Index	AMSR-E Soil moisture	$(SM_i - SM_{min})/(SM_{max} - SM_{min})$	0.25°	(Rhee et al. 2010)
PCI	2013	Meteorological drought	TRMM precipitation	$(TRMM_i - TRMM_{min})/(TRMM_{max} - TRMM_{min})$	0.25°	(Zhang and Jia 2013)
SDI	2013	Agricultural drought	TCI, PCI, VCI	PCA	0.25°	(Du et al. 2013)
SDCI	2013	Agricultural drought	TCI, PCI, VCI	Empirical weighting	0.25°	(Rhee et al. 2010)
MIDI	2013	Meteorological drought	TCI, SMCI, PCI	Empirical weighting	0.25°	(Zhang and Jia 2013)
OMDI	2015	Meteorological drought	TCI, SMCI, PCI	Constrained optimization	0.25°	(Hao et al. 2015)
OVDI	2015	Agricultural drought	TCI, SMCI, PCI, VCI	Constrained optimization	0.25°	(Hao et al. 2015)
SIF	2007	Vegetation Index	GOME-2	Radiative transfer model together with PCA	0.5°	(Guanter et al. 2007, 2012)
NIRv	2017	Vegetation Index	MODIS	The product of NDVI and NIR reflectance	500 m	(Badgley et al. 2017)
VOD	2008	Vegetation Index	TRMM	Land Parameter Retrieval Model (LPRM)	0.25°	(Owe et al. 2008)
VPD	2016	Meteorological drought	Air temperature (T) and relative humidity (RH)	$\left(1 - {}^{RH}/_{100}\right) 610.7 e^{17.4 \times T/(1.93+T)}$		(Kimball 2016)
MCDI	2020	Agricultural drought/meteorological drought	TCI, VCI, PCI, SMCI	Multivariate linear regression		(Liu et al. 2020)
PDAI	2017	Agricultural drought	Precipitation, soil moisture, NDVI	Evolution process-based multisensor collaboration (EPMC)	0.25°	(Zhang et al. 2017)
GIIDI	2019	Meteorological drought	TCI, VCI, PCI, SMCI	GWR and PCA	0.25°	(Jiao et al. 2019b)
TVPDI	2020	Agricultural drought	TCI, VCI, PCI	Euclidean distance method	0.25°	(Wei et al. 2020)
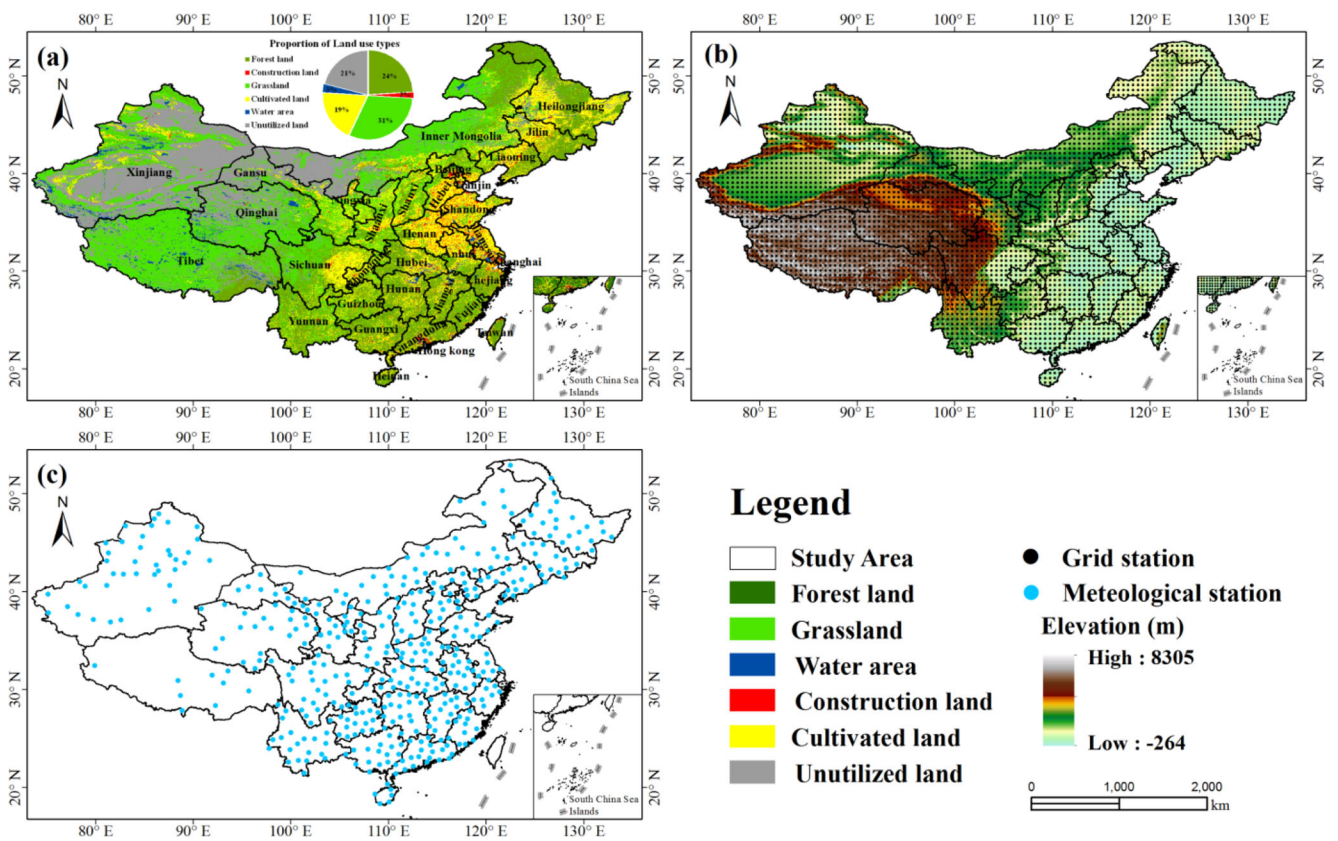
Fig. 1 Land use across China (**a**), spatial distribution of CRU gridded points and elevation (**b**), and distribution of meteorological stations in China (**c**)

China's SPI, and the time coverage is from 1960 to 2011. This study also used the product data of CRU_scPDSI; the time coverage is 1960–2011, and the spatial resolution is 0.5° × 0.5°. These data were used to verify the drought index. Figure 1b shows the grid point distribution.

Measured precipitation data

The monthly precipitation and evapotranspiration data from 2002 to 2011 are from the China Meteorological Data Network (http://data.cma.cn/), and they include observation records from national and local weather stations (450 in total) (Fig. 1c). These data were used to calculate the SPI and SPEI to determine the weights of the OMDI and OVDI (Hao et al. 2015).

Other data

The spatial resolution of the digital elevation model (DEM) data is 1 km × 1 km, and the data were from the geospatial data cloud platform (http://www.gscloud.cn) and stitched together after downloading.

The land use data are based on the current land use classification standard (GB/T21010-2011) combined with the actual situation in China; after visual interpretation, land use was divided into forestland, grassland, water areas, cultivated land,

construction land, and unutilized land (He et al. 2017). The classification results are verified with reference to Google Earth high-resolution remote sensing images and GPS field survey samples to meet research needs. The data come from the website of the Resource and Environmental Science Data Center of the Chinese Academy of Sciences (http://www.resdc.cn/data.aspx?DATAID=97), and the spatial resolution is 1 km.

Method

In situ drought indices

The SPI is the most widely used and recognized index in drought monitoring, and it is usually used to verify other indices (Um et al. 2018; Park et al. 2017; Zhang and Jia 2013). The SPI was developed by McKee et al. (1993) to quantify precipitation over multiple time scales. This index requires long-term precipitation records, and the recommended drought monitoring period is at least 50 years (Guttman 1999). Since the calculation of the SPI is based on observations from stations, the spatial distribution of the SPI is affected by the density and distribution of stations. In this study, the basic SPI data were improved, and CRU grid data were used to capture spatial details. Monthly precipitation data from

1960 to 2011 were used to establish SPI series of 1, 2, 3, 6, 9, 12, and 24 months at various weather stations. The 1-month SPI is used to analyze meteorological drought (Caccamo et al. 2011), while the 3-month or 6-month SPI seasonal scale is considered more suitable for measuring agricultural drought (Guttman 1998; Hayes et al. 1999). Meteorological droughts and agricultural droughts are usually considered short-term droughts (Brown et al. 2008). The 1-month and 3-month SPIs of the regional weather stations were averaged to estimate the regional drought. Only the data during the growing season were used in the analysis.

SPI is an indicator of the probability of occurrence of rainfall in a certain period of time. It uses г distribution probability to describe the change in precipitation and normalizes the precipitation of skewed probability distribution (Park et al. 2017; Um et al. 2018). The SPI calculation formula is as follows:

$$SPI = S \frac{t - (c_2 t + c_1)t + c_0}{[(d_3 t + d_2)t + d_1]t + 1.0} \qquad (1)$$

In the formula, $t = \sqrt{In \frac{1}{G(x)^2}}$, where $G(x)$ is the distribution probability of precipitation related to the г function, x is the precipitation sample, and S is the positive and negative coefficient of probability density.

When $G(x) > 0.5$, $S = 1$; when $G(x) \leq 0.5$, $S = -1$. $G(x)$ is calculated by the probability density integral formula of г distribution function:

$$G(x) = \frac{1}{\beta^\gamma \Gamma(x)_0} \int_0^x x^{\gamma-1} e^{\frac{-x}{\beta}} dx \qquad x > 0 \qquad (2)$$

In the formula, γ and β are the shape and scale parameters of the г distribution function, respectively. The calculation parameters are as follows: $c_0 = 2.515517$, $c_1 = 0.802853$, $c_2 = 0.010328$, $d_1 = 1.432788$, $d_2 = 0.189269$, and $d_3 = 0.001308$.

Single indices

This study defines the VCI, TCI, TCI_VUA, PCI, and SMCI as single indices. In many studies of drought indices, the VCI, TCI, TCI_VUA, PCI, and SMCI have been used (Du et al. 2013; Kogan 1995; Seiler et al. 1998; Zhang and Jia 2013). The calculation formulas are shown in Table 2. The drought index value is scaled to a range of 0 to 1. A scale value of 0 represents the driest state, and 1 represents the wettest state (Table 3).

Combined drought indices

In this study, the SDI, SDCI, MIDI, OVDI, and OMDI were defined as combined indices. The SDI, SDCI, and OVDI are

agricultural drought indices, and the OMDI and MIDI are meteorological drought indices.

SDI

The SDI was proposed by Du et al. (2013), and it combines the PCI, VCI, and TCI. The principal component analysis (PCA) method is used to extract the main information from the PCI, VCI, and TCI and eliminate the relevant signals (Deng et al. 2008). The principal component transformation is completed in the ENVI software environment. Each month of PCI, VCI, and TCI data was input as bands, and the PCA method was used to calculate the bands. The first principal component (PC1) contains more than 75% of the information from the PCI, VCI, and TCI. Based on the PCA method, the SDI dataset from June 2002 to October 2011 was generated. The SDI was divided into five categories according to the classification displayed in Table 4.

SDCI

We used the empirical weight method to combine the VCI, TCI, and PCI to establish the SDCI (Rhee et al. 2010). To obtain the best weighted components of the SDCI in China, several sets of weights were tested for the SDCI and SPI for 7 time scales (1, 2, 3, 6, 9, 12, and 24 months) in China (Table 5). In all cases, the SDCI showed the highest correlation with the 1-month-scale SPI. According to the performance of the SDCI under different weight combinations, a VCI of 0.1, a TCI of 0.4, and a PCI of 0.5 are the best combination of components of the SDCI in the study area.

MIDI

The MIDI was established by Zhang and Jia (2013). The aim is to monitor short-term drought conditions and integrate three variables: TRMM-based precipitation data, AMSR-E-based SM, and AMSR-E surface temperature data. To obtain the best MIDI weight distribution for China, this study assumes many experience-based weight distributions. The MIDI values calculated from these experience-based weight distributions were compared with the results of the scPDSI and SPI in China for Pearson correlation analysis. All correlations in this study were statistically significant ($p < 0.01$). The results show that the weighted MIDI has a strong correlation with SPI-1, and the correlation decreases as the SPI time scale increases (Table 6). From the test results, the MIDI when the weights of the PCI, SMCI, and TCI are 0.5, 0.3, and 0.2, respectively, shows the best correlation with the scPDSI and SPI of each time scale. This combined drought index is used to assess the capability of remote sensing drought monitoring in China.

Table 2 Descriptions of remote sensing-based single condition drought indices, including names, data sources, calculated formulas, and reference

Drought index	Data source	Formula	Reference
VCI	MODIS	$(NDVI_i - NDVI_{min})/(NDVI_{max} - NDVI_{min})$	(Kogan 1995; Du et al. 2013)
TCI	MODIS, AMSR-E	$(LST_{max} - LST_i)/(LST_{max} - LST_{min})$	(Kogan 1995; Wu et al. 2013)
PCI	TRMM	$(TRMM_i - TRMM_{min})/(TRMM_{max} - TRMM_{min})$	(Zhang and Jia 2013; Rhee et al. 2010)
SMCI	AMSR-E	$(SM_i - SM_{min})/(SM_{max} - SM_{min})$	(Zhang and Jia 2013; Hao et al. 2015)

The MIDI is calculated by the following formula:

$$MIDI = \alpha \times PCI + \beta \times SMCI + (1-\alpha-\beta) \times TCI \quad (3)$$

OVDI and OMDI

The OVDI and OMDI are combined drought indices, which are optimal weight combinations of the four variables of precipitation, SM, vegetation status, and surface temperature. However, there are obvious spatial differences in climatic factors such as precipitation and temperature, so the combined values of the OVDI and OMDI weights calculated for different regions may be different (Powell 1978). The constrained optimization method is used to optimize the parameters of remote sensing variables; that is, under the constraints of these variables, they are combined by maximizing the correlation with the in situ indices of certain variables (Powell 1983). The PCI, TCI, VCI, and SMCI were combined to calculate the OVDI and OMDI, taking the SPI as reference data. In this study, to calculate the OVDI and OMDI, we used data from 450 observing stations to calculate the SPI and SPEI (Fig. 1c). For detailed information about the OVDI and OMDI calculations, please refer to Hao et al. (2015).

The optimization weight method is described by the following formula:

$$f(x,y) = \max\left(\frac{E[(X-ux) \times (Y-uy)]}{\partial x \times \partial y}\right) \quad (4)$$

$$X = \begin{cases} SPI \\ SPEI \end{cases} \quad (5)$$

$$Y = \begin{cases} \alpha \times TCI + \beta \times PCI + (1-\alpha-\beta) \times SMCI \\ \alpha \times TCI + \beta \times PCI + \gamma \times SMCI + (1-\alpha-\beta) \times VCI \end{cases} \quad (6)$$

The formula is subject to the constraints

$$\begin{aligned} 0 &< \alpha < 1 \\ 0 &< \beta < 1 \\ 0 &< \gamma < 1 \end{aligned} \quad (7)$$

In the formula, $f(x, y)$ represents the situation with the greatest correlation between X and Y, X represents the SPI and SPEI, and Y represents the OVDI and OMDI. The OVDI is a combination of the TCI, PCI, SMCI, and VCI. The OMDI is a combination of the TCI, PCI, and SMCI. ∂x and uy are the standard deviations of the variables X and Y, respectively; ux and uy are the mean values of the variables X and Y, respectively; and α, β, and γ are the optimized parameters of the TCI, PCI, and SMCI, respectively.

The constrained optimization method is used to analyze the correlation between China's SPI and SPEI and each single drought index based on remote sensing (PCI, SMCI, TCI, and VCI). The weights of the TCI, PCI, and SMCI of OMDI are 0.14, 0.53, and 0.33, respectively. The weights of the TCI, PCI, SMCI, and VCI are 0.43, 0.11, 0.13, and 0.33, respectively.

Pearson correlation analyses

A correlation analysis is a statistical method that reflects the degree of correlation between variables (Mitchell et al. 2008). In geographic research, the Pearson correlation coefficient is usually used to test the relationships and accuracy of various indices. The calculation formula is as follows:

Table 3 Combined-index information on establishment methods and data sources

Drought index	Drought type	Data source	Single drought indices based	Weight determination method	Source
SDI	Agricultural	MODIS, TRMM	TCI, PCI, VCI	PCA	(Du et al. 2013)
SDCI	Agricultural	MODIS, TRMM, AMSR-E	TCI, PCI, VCI	Empirical weights	(Rhee et al. 2010)
MIDI	Meteorological	MODIS, TRMM, AMSR-E	TCI, PCI, SMCI	Empirical weights	(Zhang and Jia 2013)
OVDI	Agricultural	MODIS, TRMM, AMSR-E	TCI, PCI, SMCI, VCI	Constrained optimization	(Hao et al. 2015)
OMDI	Meteorological	MODIS, TRMM, AMSR-E	TCI, PCI, SMCI	Constrained optimization	(Hao et al. 2015)

Table 4 Classification of the drought indices compared in this study

Name of class	PCI	TCI	VCI	SMCI	MIDI	OMDI	SDCI	SDI	OVDI
Extreme drought	0–0.1	0–0.1	0–0.1	0–0.1	0–0.1	0–0.2	0–0.2	0–0.2	0–0.2
Severe drought	0.1–0.2	0.1–0.2	0.1–0.2	0.1–0.2	0.1–0.2	0.2–0.4	0.2–0.3	0.2–0.3	0.2–0.4
Moderate drought	0.2–0.3	0.2–0.3	0.2–0.3	0.2–0.3	0.2–0.3	0.4–0.6	0.3–0.4	0.3–0.4	0.4–0.6
Mild drought	0.3–0.4	0.3–0.4	0.3–0.4	0.3–0.4	0.3–0.4	0.6–0.8	0.4–0.5	0.4–0.5	0.6–0.8
No drought	0.5–1	0.5–1	0.5–1	0.5–1	0.4–1	0.8–1	0.5–1	0.5–1	0.8–1

The names of the category rows show different definitions of drought severity, and all other rows include drought indices

$$R_{xy} = \frac{\sum_{i=1}^{n}\left(x_i - \overline{x}\right)\left(y_i - \overline{y}\right)}{\sqrt{\sum_{i=1}^{n}\left(x_i - \overline{x}\right)^2 \sum_{i=1}^{n}\left(y_i - \overline{y}\right)^2}} \qquad (8)$$

In the formula, x_i and $\overline{x}$ are the i-th value and average value of the variable X, respectively; y_i and $\overline{y}$ are the i-th value and average value of the variable Y, respectively. n is the total number of sample sequences. The closer $|R|$ is to 1, the stronger the correlation. If $R = \pm 1$, the two groups of variables have a perfect positive (negative) correlation. If $0 < R < 1$, the two groups of variables are positively correlated; if $-1 < R < 0$, then the two groups of variables are negatively correlated (Shen et al. 2019).

Results

Spatial distribution patterns of remote sensing drought indices

Spatial distribution patterns of single drought indices

After consulting the China Statistical Yearbook, we found that severe droughts occurred in 2009 and 2011 (NBSC 2009, 2011). The drought indices in July 2009 presented in Fig. 2

a, b, c, d, and e and those in July 2011 presented in Fig. 3 a, b, c, d, and e show the changes in the single indices and allow a comparison of these indices in these 2 months.

Figure 2 shows the spatial distributions of the drought levels in July 2009 characterized by five indices: the PCI, VCI, TCI_VUA, TCI, and SMCI. The PCI distribution indicates that Northwest China is the driest area, while the southeast, southwest, and south are the wettest areas. The VCI and SMCI have similar spatial distributions, both of which demonstrate severe drought in the northwest, including most of Inner Mongolia, Xinjiang, Tibet, and Qinghai; however, the northeastern, southwestern, and southern regions are relatively wet. The distributions of the TCI and TCI_VUA vary significantly in space, especially in Qinghai and Tibet: the severe drought in Qinghai and Tibet was monitored by the TCI_VUA, while the MODIS-derived TCI can monitor droughts and identify severe droughts in small areas throughout China.

Similarly, the spatial distributions of the drought grades represented by these five single drought indices in July 2011 are shown in Fig. 3. Each single drought index has a similar distribution spatial to that in July 2009. The difference is that the PCI detected extreme drought events in the northwestern desert region, while severe drought events occurred in Hunan Province. The VCI and SMCI distributions indicate that Northwest China and Tibet are arid areas, while the

Table 5 Correlation coefficients among the SDCI and scPDSI and SPI at different time scales

Indices	Weights			$n = 15{,}405$							
	VCI	TCI	PCI	PDSI	SPI-1	SPI-2	SPI-3	SPI-6	SPI-9	SPI-12	SPI-24
SDCI	0.4	0.3	0.3	0.422[**]	0.494[**]	0.448[**]	0.342[**]	0.331[**]	0.316[*]	0.262[*]	0.255[*]
	0.5	0.2	0.3	0.416[**]	0.472[**]	0.325[**]	0.322[*]	0.334[**]	0.321[*]	0.261[*]	0.256[*]
	0.3	0.3	0.4	0.444[**]	0.544[**]	0.485[**]	0.374[**]	0.347[**]	0.327[**]	0.272[*]	0.261[*]
	0.2	0.3	0.5	0.466[**]	0.594[**]	0.523[**]	0.507[**]	0.462[**]	0.437[**]	0.382[**]	0.367[**]
	0.1	0.4	0.5	*0.474*[**]	*0.608*[**]	*0.551*[**]	**0.531**[**]	0.457[**]	0.425[**]	*0.383*[**]	0.365[**]
	0.4	0.1	0.5	0.449[**]	0.544[**]	0.466[**]	0.456[**]	*0.468*[**]	*0.447*[**]	0.378[**]	*0.368*[**]

[**] Denotes a significant correlation at the 0.01 confidence level

[*] Denotes a significant correlation at the 0.05 confidence level

The highest r values of each combined drought index for each row/column were shown in italics/bold

Table 6 Correlation coefficients among the MIDI and scPDSI and SPI at different time scales

Indices	Weights			$n = 15{,}405$							
	PCI	SMCI	TCI	PDSI	SPI-1	SPI-2	SPI-3	SPI-6	SPI-9	SPI-12	SPI-24
MIDI	0.3	0.4	0.3	0.325**	0.449**	0.406**	0.410**	0.373**	0.292*	0.249**	0.226*
	0.3	0.5	0.2	0.296*	0.41**	0.366**	0.374**	0.363**	0.290*	0.23**	0.218*
	0.4	0.3	0.3	0.355**	0.501**	0.442**	0.439**	0.390**	0.307*	0.267*	0.223*
	0.4	0.4	0.2	0.326**	0.461**	0.401**	0.402**	0.382**	0.305*	0.246*	0.233*
	0.4	0.5	0.1	0.367**	0.519**	0.360**	0.365**	0.368**	0.301*	0.229*	0.22*
	0.5	0.3	0.2	*0.395**	*0.604**	*0.495**	*0.464**	0.382**	*0.364**	*0.313**	0.235*
	0.5	0.4	0.1	0.36**	0.562**	0.388**	0.387**	*0.383**	0.314**	0.243*	*0.249*

** Denotes a significant correlation at the 0.01 confidence level

* Denotes a significant correlation at the 0.05 confidence level

TCI_VUA shows that most of the central region is not arid and presents the greatest difference from the other single drought indices in Tibet and China. In general, the drought situations monitored by these five indices feature different spatial variabilities in Qinghai, Tibet, Hunan, Guizhou, and Heilongjiang.

### Spatial distribution patterns of combined drought indices

Among the combined drought indices, there are significant differences between the meteorological drought indices and the agricultural drought indices, suggesting that combined drought indices can distinguish between meteorological drought and agricultural drought. Compared with the agricultural drought indices, the meteorological drought indices show that more areas are in an arid state. Two of the agricultural drought indices, namely, the SDCI and OVDI, do not show a large area of overlap in the southern part of China. The same situation can be found for the meteorological drought indices, the MIDI and OMDI. In contrast, the SDCI, SDI, and OVDI show a high degree of consistency. Almost all the drought indices considered are able to monitor the drought situation in Northwest China.

In July 2009, the five combined drought indices (MIDI, OMDI, OVDI, SDCI, and SDI) exhibit similar spatial
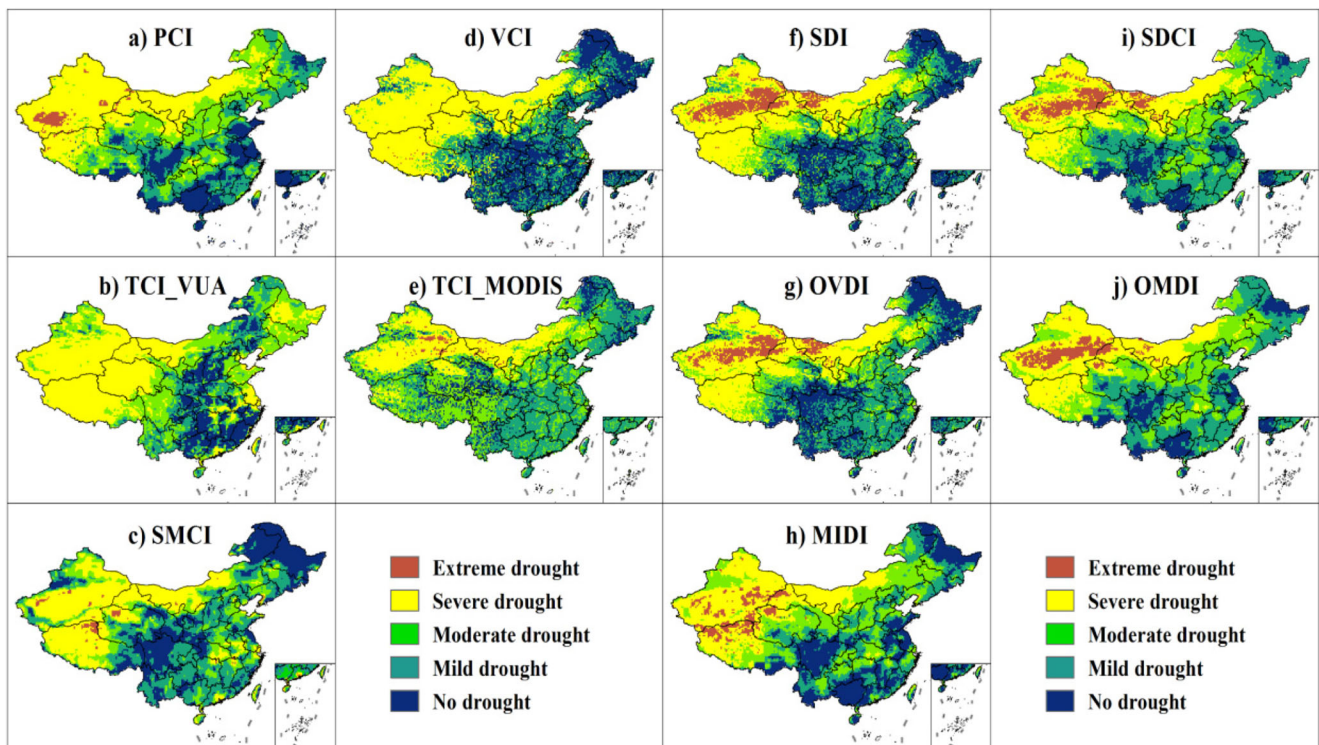
Fig. 2 Drought conditions in China monitored by multiple drought indices in July 2009
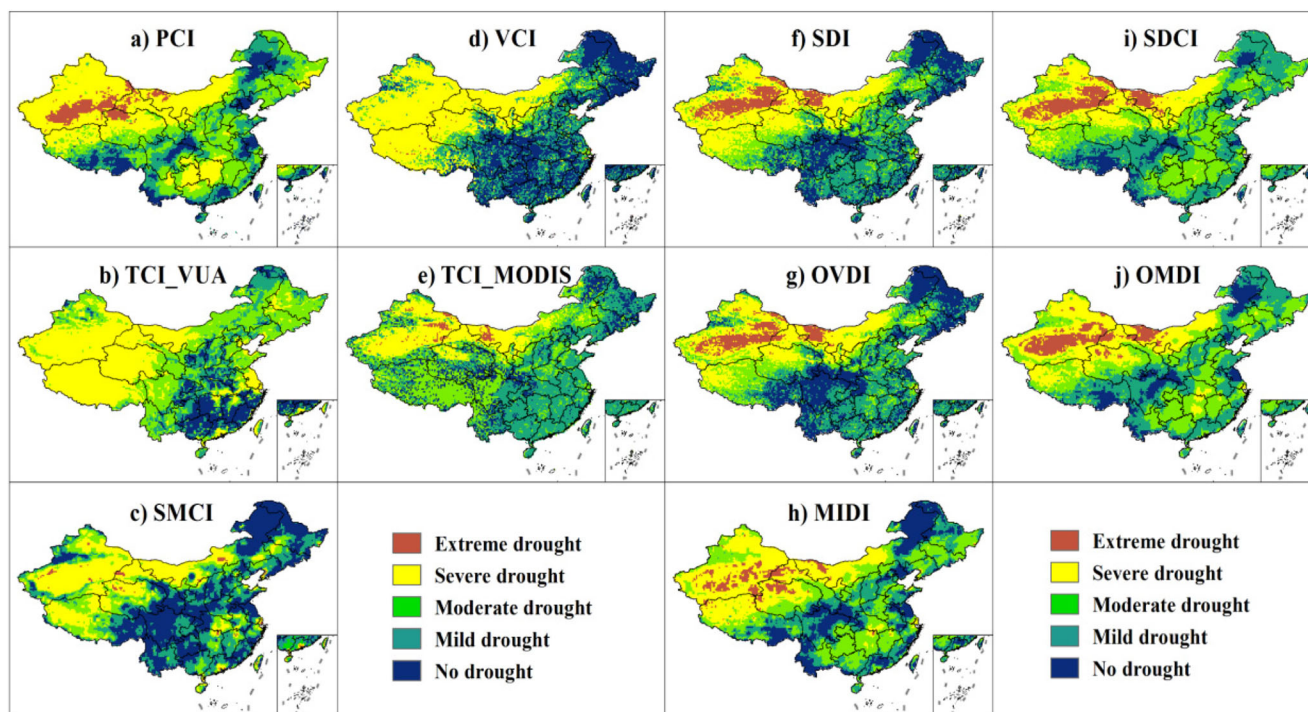
Fig. 3 Drought conditions in China monitored by multiple drought indices in July 2011

distribution characteristics. In Fig. 2 f, g, h, i, and j, the spatial distributions of the drought grades of the meteorological drought indices (MIDI and OMDI) are highly consistent, and both indices monitor severe drought events in central China. For the drought grade distributions of the agricultural drought indices (the OVDI, SDCI, and SDI), the OVDI and SDCI display almost identical spatial distributions, and both indices monitor extreme drought events in the northwestern desert region and severe drought events in western Xinjiang and eastern Inner Mongolia, while both the southwestern and northeastern regions are relatively wet. Similarly, Fig. 3 f, g, h, i, and j show the spatial distributions of the MIDI, OMDI, OVDI, SDCI, and SDI in July 2011. The MIDI, OMDI, and SDCI have high spatial consistency and monitor severe drought in the south. The OVDI and SDI also exhibit high compliance. However, the PCI, VCI, TCI, and SMCI in southwestern China show different drought situations, while the combined drought indices (SDI and OVDI) show similar drought situations.
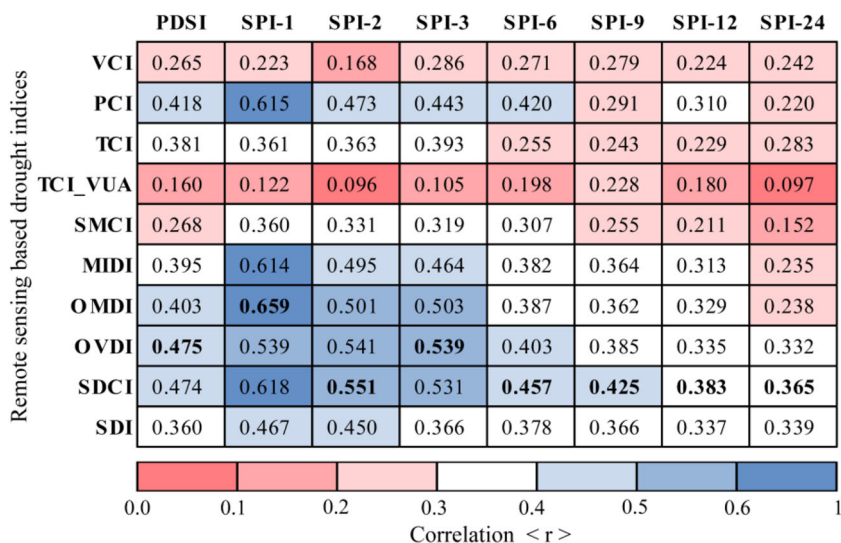
Comparison of remote sensing drought indices

According to the similarity of the drought indices, we can determine the drought status of different regions. Figure 4 and Fig. 5 show maps describing the temporal and spatial similarities between the drought indices and the in situ drought index based on the linear correlations between the drought indices.

Comparison between the single drought indices

The correlation coefficients (r) between the single indices and the in situ drought index are illustrated in Fig. 4. The correlation between the MODIS-derived VCI and the in situ drought index is relatively good overall, where the former performs best for SPI-3 and SPI-6 but is inferior for SPI-9, SPI-12, and SPI-24. As shown in Fig. 5, the VCI and the in situ drought index show a strong correlation, representing the strongest correlation in central China. The correlations between the VCI and SPI-6 and SPI-9 are high in the northeast. The highest correlation corresponds to forestland, while the weakest is observed for cultivated land. Generally, areas with a stable VCI have higher annual precipitation, including mainly forestland and grassland areas. Compared with the other indices, the correlation of the VCI in wet areas (such as the southern and coastal areas) is weak, whereas in the northwestern arid region, the VCI outperforms the other single indices.

The PCI has relatively strong correlations with SPI-1 and SPI-3 (with average coefficients of 0.615 and 0.443, respectively). The regions with the highest correlations are located in southern China. The PCI performs slightly better in short-term drought monitoring than the other indices (Fig. 5), and the PCI has a stronger correlation with SPI-1 in almost all of China. In addition, the correlation between the PCI and SPI-3 is stronger than those between the VCI, TCI, and SMCI and SPI-3 in most regions. However, also in most regions, the correlation between the PCI and SPI-9 is lower than those between the VCI, TCI, and SMCI and SPI-9.

Fig. 4 Correlation coefficients (*r*) between remote sensing drought indices (rows) and station-based drought indices (columns)

	PDSI	SPI-1	SPI-2	SPI-3	SPI-6	SPI-9	SPI-12	SPI-24
VCI	0.265	0.223	0.168	0.286	0.271	0.279	0.224	0.242
PCI	0.418	0.615	0.473	0.443	0.420	0.291	0.310	0.220
TCI	0.381	0.361	0.363	0.393	0.255	0.243	0.229	0.283
TCI_VUA	0.160	0.122	0.096	0.105	0.198	0.228	0.180	0.097
SMCI	0.268	0.360	0.331	0.319	0.307	0.255	0.211	0.152
MIDI	0.395	0.614	0.495	0.464	0.382	0.364	0.313	0.235
OMDI	0.403	**0.659**	0.501	0.503	0.387	0.362	0.329	0.238
OVDI	**0.475**	0.539	0.541	**0.539**	0.403	0.385	0.335	0.332
SDCI	0.474	0.618	**0.551**	0.531	**0.457**	**0.425**	**0.383**	**0.365**
SDI	0.360	0.467	0.450	0.366	0.378	0.366	0.337	0.339

Remote sensing based drought indices

0.0   0.1   0.2   0.3   0.4   0.5   0.6   1
Correlation < r >

As depicted in Fig. 4, the MODIS-derived TCI is superior to the VUA-derived TCI in monitoring short-term drought, confirming that the choice of the single drought index is very important when establishing a combined drought index. In general, the MODIS-derived TCI is better for monitoring drought on a short time scale. Compared with the TCI_VUA, the MODIS-derived TCI has a stronger correlation with the in situ drought index in almost all of China. It is important to note that the MODIS-derived TCI and VUA-derived TCI have similar spatial variabilities, and both single indices have a good correlation with SPI-3 and are highly suitable for long-term drought monitoring.

The correlation between the SMCI derived from the VUA and in situ drought index SPI-1 is relatively good with a correlation coefficient of 0.360. However, the correlations between the PDSI and the long-term SPI and SMCI are weak in most regions. The SMCI is more suitable for monitoring short-term drought conditions in large areas. Moreover, compared with the VCI, PCI, and TCI, the SMCI is particularly sensitive to terrain; the SMCI is calculated from soil moisture, so the land type affects the value of the SMCI. Figure 1a and Fig. 5 show that the *r* values between the SMCI and SPI-1 and SPI-3 are lower in areas with more forestland coverage; for example, in the Northeast Greater Khingan Range and Xinjiang Tianshan, the *r* values are lower than those of cultivated land and grassland in central China. In areas with limited forestland coverage and sparse vegetation, the correlation between the SMCI and SPI-1 is higher than that between the TCI and SPI-1.

In general, different single indices have specific characteristics. The PCI has the highest correlation with the in situ drought index, followed by the TCI derived from MODIS. The PCI is highly correlated in most regions, while the SMCI is more suitable for short-term drought monitoring.

Comparison between single drought indices and combined drought indices

The combined drought indices have advantages over the single drought indices. When all drought indices are correlated with SPI-1, the overall correlation coefficient of a combined drought index is higher than that of a single drought index. However, the correlation coefficient between the PCI (a single drought index) and SPI-1 is also relatively high. Among the meteorological drought indices, the correlation between the PCI and SPI-1 is 0.615, and the correlation between the MIDI and SPI-1 is 0.601; thus, the *r* value of the MIDI for the combined drought index is lower than that of the PCI for the single drought index. The correlation between the OMDI and SPI-1 is 0.659, and the *r* value of the OMDI for the combined drought index is slightly higher than the *r* value of the PCI for the single drought index. In terms of the agricultural drought indices, the *r* values of the OVDI with the SDCI and SPI-3 are 0.539 and 0.531, respectively, while the *r* values of the PCI with the TCI and SPI-3 are only 0.443 and 0.393, respectively.

Comparison of combined drought indices

Generally, a combined drought index is a type of synthesis method. The correlation between the in situ drought index and each combined drought index shows the lack of an obvious difference among the combined drought indices. However, combined drought indices have some shortcomings. Figure 4 shows that most of the combined drought indices are highly correlated with SPI-1 and SPI-2. We define the MIDI and OMDI as meteorological drought indices. The correlations of the MIDI and OMDI with SPI-1 are high and should be close to those for the short-term drought indices. Therefore, the MIDI and OMDI are suitable for short-term
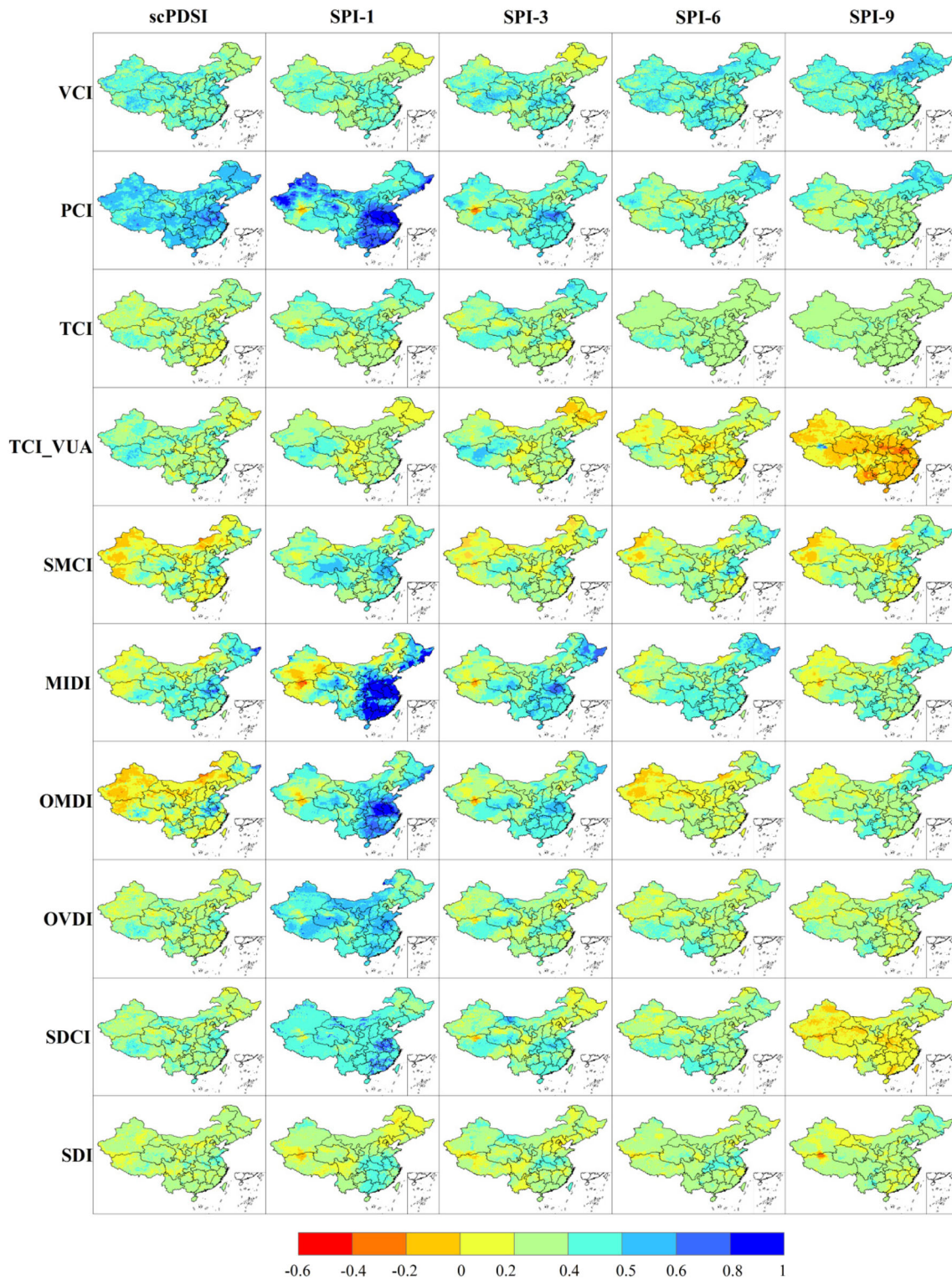
Fig. 5 Coefficient of determination of temporal correlation between monthly maps of remote sensing-based combined drought indices and in situ station-based drought indices

drought monitoring. Related research defines the OVDI, SDCI, and SDI as agricultural drought indices; the changes in the r values of most combined agricultural drought indices with SPI-3 are larger than those of the short-term drought

indices (Fig. 4). The correlation of the in situ drought index with the OMDI is higher than that with the MIDI, demonstrating that the constrained optimization method has certain advantages when combining single drought indices. Among the

agricultural drought indices, the SDCI has the highest correlation with the in situ drought index; on the other hand, the SDCI uses the empirical weighting calculation of the VCI, TCI, and PCI, and the weight of the PCI is greater than the weights of the TCI and VCI. This finding shows that the influence of the empirical weighting method should be fully considered. The SDCI and SDI are based on the same single index, but while the SDI is constructed by PCA, the SDCI is constructed by the empirical weighting method. At the same time, both the SDCI and the SDI are indices for monitoring agricultural drought, and the correlation of the in situ drought index with the SDCI is higher than that with the SDI. This finding indicates that performing PCA on VCI, TCI, and PCI data will cause a loss of information during the dimensionality reduction process, resulting in a low correlation with the in situ drought index.

As shown in Fig. 5, the combined indices have similar spatial variabilities. For the agricultural drought indices, the spatial variability does not differ greatly among the OVDI, SDCI, and SDI; in particular, their correlations with SPI-6 and SPI-9 are the same. In the northwestern arid area, the correlations of the MIDI and OMDI with SPI-1 are relatively low (approximately between − 0.2 and 0.3) but reach 0.5–0.8 in the central and southern regions. These correlations present a predominant trend of high in the southern region and low in the western region. The correlations between the MIDI and OMDI and SPI-3, SPI-6, and SPI-9 also have similar spatial distributions. Only the OMDI shows a stronger correlation with SPI-1. The three agricultural drought indices (OVDI, SDCI, and SDI) show relatively small spatial differences, and the correlation among their spatial distributions is relatively even overall.

Discussion

Single index selection

The selection of single indices has a decisive effect on the combined index, and different combined indices have different data requirements. Hence, different characteristics are considered when using various methods to quantify drought. For

example, although the OMDI and OVDI use the same combination method (constrained optimization method), because they employ different single indices, they show different drought distributions and characteristics. Furthermore, the SDCI and SDI use the same single indices (the VCI, TCI, and PCI) to monitor agricultural drought.

We now analyze the meteorological drought indices. The PCI is the most important single index in the OMDI, while the weights of the TCI and SMCI are relatively low. The weight of the PCI in the OMDI is 0.53, while the weights of the TCI and SMCI are 0.14 and 0.33, respectively. These results show that the TCI and SMCI contribute less to the OMDI. Figure 4 shows that the correlations between the OMDI and PCI and the in situ drought index are similar. The OMDI's r value is 0.044 higher than that of the PCI. The MIDI is another meteorological drought index, in which the weights of the PCI, SMCI, and TCI are 0.5, 0.3, and 0.2, respectively. In meteorological drought monitoring, the PCI, which has the highest weight, is the most effective. Compared with the PCI, the PCI-merged MIDI is more complicated, but it contains little additional information, and there is no substantial improvement. Thus, in certain situations, a single index can be more advantageous than a combined drought index; if a single index performs better than other single indices, the weight of that single index will be the highest when constructing a combined drought index, and the performance of the combined index will not differ significantly from that of the single index. In contrast, the OVDI is a combined agricultural drought index composed of the TCI and VCI, whose weights are 0.43 and 0.33, respectively, indicating that the degree of vegetation coverage and surface temperature play important roles. Moreover, the correlation between the OVDI and SPI-1 reaches 0.539, while the correlations of the TCI and VCI with SPI-1 are only 0.361 and 0.223, respectively. These results show that the combined drought index is somewhat improved over the single indices that compose it.

Long-term evolution characteristics of drought indices

Combining five combined drought indices, we analyzed the long-term evolutionary characteristics of China's regional dry

Fig. 6 Annual time series of various drought indices in China from 2002 to 2011
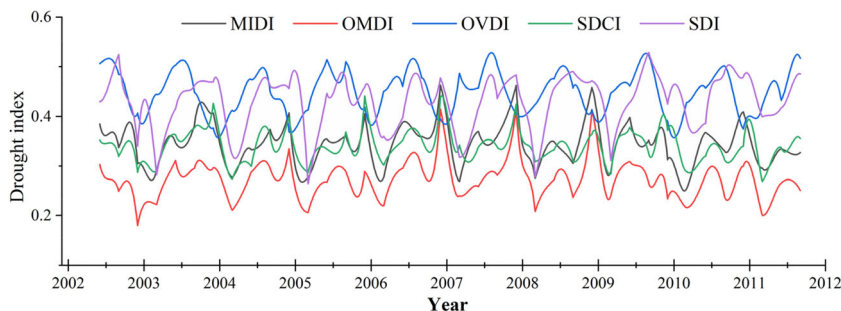
Table 7 Correlation coefficients among the combined drought indices

Drought index	MIDI	OMDI	OVDI	SDCI
MIDI	–	–	–	–
OMDI	0.826**	–	–	–
OVDI	0.417**	0.547**	–	–
SDCI	0.646**	0.848**	0.583**	–
SDI	0.469**	0.525**	0.638**	0.484**

and wet changes from June 2002 to October 2011. As shown in Fig. 6, in the overall change trend over time, the MIDI and OMDI both have good spatial consistency, and their temporal change trends are almost the same. The MIDI and OMDI are both meteorological drought indices with the same three single indices (the PCI, TCI, and SMCI); the difference between the two is that different methods are used for their construction: the OMDI adopts the constrained optimization method, while the MIDI adopts the empirical weighting method. In addition, the temporal trends of the MIDI and SDCI are similar, whereas the OVDI and SDI have slight deviations from other combined drought indices.

Correlations between combined drought indices

The MIDI, OMDI, OVDI, SDCI, and SDI are all very effective indices for monitoring drought. The differences among these drought indices are that different modeling methods are used when constructing them, and different factors that cause droughts (e.g., precipitation, soil moisture, land surface temperature, and vegetation conditions) are considered. According to the spatial correlations between the drought indices in Fig. 7, both the OMDI and the SDCI have a high degree of spatial correlation in China as a whole with a correlation coefficient of 0.848. Moreover, the MIDI and OMDI are generally highly correlated with a correlation coefficient of 0.826. The spatial correlations between the MIDI and OVDI

and between the MIDI and SDI are the poorest with correlation coefficients of 0.417 and 0.469, respectively. The spatial correlation between the SDCI and SDI is also low overall, reaching a coefficient of 0.484. The reason for this result may be that the combined factors considered in each drought index are different. On the other hand, among the combined drought indices, the different combination methods are another key factor. For example, the OMDI and SDCI are highly spatially correlated, but their combination methods are different. We used the constrained optimization and empirical weighting methods to obtain the OMDI and SDCI, respectively, but the performance of the indices is similar. In contrast, the OMDI and MIDI have similar spatial distributions. Therefore, it is very important to summarize the combined drought indices in different regions with simple methods and efficient monitoring results (Table 7).

Influencing factors

From the correlation diagrams between each drought index and the in situ drought index (Fig. 5), the MODIS-derived VCI and the MODIS-derived TCI have similar spatial variabilities, which is because these indices use data from the same satellite sensors, and the NDVI and LST data inputs cover the same geographic area and time frame. There is a strong negative correlation between the LST and NDVI (Karnieli et al. 2010), which has been confirmed by many previous studies. Because of this correlation, the LST and NDVI may behave similarly for the same land cover. In addition, the PCI has a high correlation with SPI-1. The PCI is determined based solely on rainfall and is not affected by changes in the surface, such as variations in the land cover, land use, and DEM. The SMCI has a high correlation with the short-term in situ drought index, while it has a weak correlation with the long-term SPI in most areas. Hence, the SMCI is more suitable for monitoring large-scale, short-term drought

Fig. 7 Spatial correlations between combined drought indices
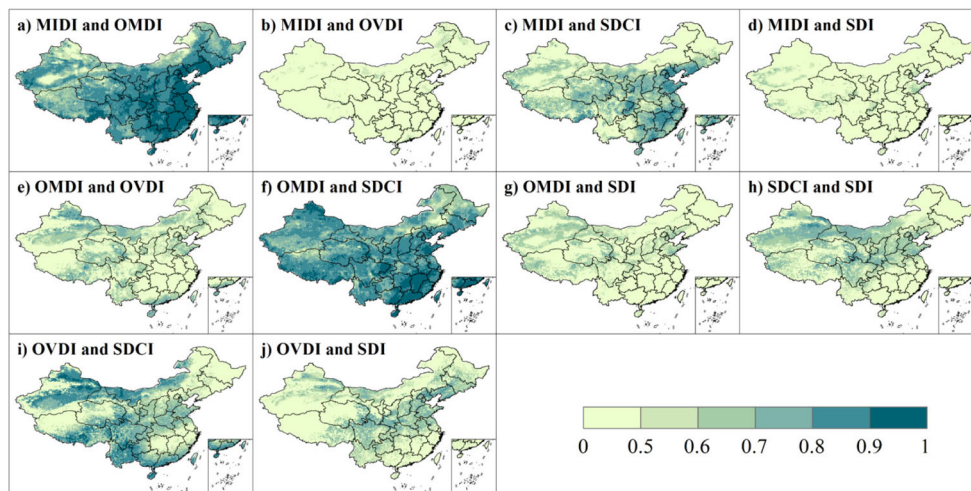
conditions. Combining Fig. 1a and Fig. 5 shows that the SMCI is more sensitive to short-term drought in areas with limited forest coverage and sparse vegetation. The SMCI is calculated based on the soil moisture retrieved from X- and C-band microwave brightness temperature data from 1 to 1.5-cm soil, so when the vegetation density is too high, the SMCI value will not achieve good convergence. Other factors also affect the performance of remote sensing drought indices. Residual cloud pollution in a remote sensing image will affect the drought results in a specific area, and the low spatial resolution of some remote sensing data means that local drought values may not be accurately monitored. Finally, human disturbances can change the agricultural climate and cause errors in drought monitoring and the actual conditions, such as the irrigation and fertilization of crops.

Conclusions

In this study, the single drought indices, combined drought indices, and in situ drought indices across China were compared over the period from 2002 to 2011. July 2009 and July 2011 were selected as typical dry years to analyze the spatial distributions of the indices. The analysis revealed different characteristics between the single drought indices and combined drought indices. The VCI derived from MODIS NDVI data was not suitable for monitoring drought in wet regions because it was easily affected by climate change. However, the VCI was more reliable than the other indices for monitoring drought in arid and semiarid regions. In addition, we found that the TCI was not suitable to monitor drought in desert environments because of interference by the LST. The SMCI could be affected by soil moisture, especially in densely forested and grassland-covered regions. The PCI was most suitable for monitoring short-term droughts because it exhibited a strong correlation with the short-term in situ drought index. The results of this comparison showed that the combined drought indices could better reflect drought events than the single indices in specific areas and could display the detailed characteristics of drought on a large scale. The empirical weighting method was more suitable than the constrained optimization method for constructing combined drought indices because of the simplicity of its theory, fewer parameters, and easier calculation process. These results may be helpful for drought monitoring on different scales, especially in agricultural regions. The evaluation framework proposed and utilized in this study can also be applied to other regions by adjusting the parameters of the model in the region of interest.

Data availability Not applicable.

Compliance with ethical standards

Competing interests The authors declare that they have no competing interests.

Ethics approval and consent to participate Not applicable.

Consent for publication Not applicable.

References

Badgley G, Field CB, Berry JA (2017) Canopy near-infrared reflectance and terrestrial photosynthesis. Sci Adv 3(3):e1602244

Badgley G, Field CB, Berry JA (2019) Terrestrial gross primary production: using NIRV to scale from site to globe. Glob Chang Biol 25(11):3731–3740

Bayarjargal Y, Karnieli A, Bayasgalan M, Khudulmur S, Gandush C, Tucker C (2006) A comparative study of NOAA–AVHRR derived drought indices using change vector analysis. Remote Sens Environ 105:9–22

Bhuiyan C, Singh RP, Kogan FN (2006) Monitoring drought dynamics in the Aravalli region (India) using different indices based on ground and remote sensing data. Int J Appl Earth Obs Geoinf 8(4):289–302

Bindlish R, Jackson TJ, Wood E, Gao HL, Starks P, Bosch D, Lakshmi V (2003) Soil moisture estimates from TRMM microwave imager observations over the southern United States. Remote Sens Environ 85(4):507–515

Brown JF, Wardlow BD, Tadesse T, Hayes MJ, Reed BC (2008) The vegetation drought response index (VegDRI): a new integrated approach for monitoring drought stress in vegetation. IEEE Geosci Remote Sens Lett 45:16–46

Buckley TN (2019) How do stomata respond to water status? New Phytol 224:21–36

Caccamo G, Chisholm LA, Bradstock RA, Puotinen ML (2011) Assessing the sensitivity of MODIS to monitor drought in high biomass ecosystems. Remote Sens Environ 115:2626–2639

De Jeu RAM, Wagner W, Holmes TRH, Dolman AJ, Van de Giesen NC, Riesen J (2008) Global soil moisture patterns observed by space borne microwave radiometers and scatterometers. Surv Geophys 29:399–420

Deng JS, Wang K, Deng YH, Qi GJ (2008) PCA-based land-use change detection and analysis using multitemporal and multisensor satellite data. Int J Remote Sens 29(16):4823–4838

Dracup JA, Lee KS, Paulson EG (1980) On the statistical characteristics of drought events. Water Resour Res 16:289–296

Draper CS, Walker JP, Steinle PJ, De Jeu RAM, Holmes RHT (2009) An evaluation of AMSR-E derived soil moisture over Australia. Remote Sens Environ 113:703–710

Du L, Tian Q, Yu T, Meng Q, Jancso T, Udvardy P, Huang Y (2013) A comprehensive drought monitoring method integrating MODIS and TRMM data. Int J Appl Earth Obs Geoinf 23:245–253

Dubovyk O, Ghazaryan G, González J, Graw V, Löw F, Schreier J (2019) Drought hazard in Kazakhstan in 2000-2016: a remote sensing perspective. Environ Monit Assess 191:510

Feng L, Li T, Yu W (2014) Cause of severe droughts in Southwest China during 1951–2010. Clim Dyn 43:2033–2042

Frankenberg C, Fisher JB, Worden J et al (2011) New global observations of the terrestrial carbon cycle from GOSAT: patterns of plant fluorescence with gross primary productivity. Geophys Res Lett 38: L17706

Gitelson AA, Kogan F, Zakarin E, Spivak L, Lebed L (1998) Using AVHRR data for quantitive estimation of vegetation conditions: calibration and validation. Adv Space Res 22(5):673–676

Guanter L, Alonso L, GómezChova L, AmorósLópez J, Vila J, Moreno J (2007) Estimation of solar induced vegetation fluorescence from space measurements. Geophys Res Lett 34:L08401

Guanter L, Frankenberg C, Dudhia A, Lewis PE, Gómez-Dans J, Kuze A, et al (2012) Retrieval and global assessment of terrestrial chlorophyll fluorescence from GOSAT space measurements. Remote Sens of Environ 121:236–251

Guanter L, Zhang Y, Jung M, Joiner J, Voigt M, Berry JA, Frankenberg C, Huete AR, Zarco-Tejada P, Lee JE, Moran MS, Ponce-Campos G, Beer C, Camps-Valls G, Buchmann N, Gianelle D, Klumpp K, Cescatti A, Baker JM, Griffis TJ (2014) Global and time-resolved monitoring of crop photosynthesis with chlorophyll fluorescence. Proc Natl Acad Sci 111(14):E1327–E1333

Guttman NB (1998) Comparing the Palmer drought index and the standardized precipitation index. J Am Water Resour As 34:113–121

Guttman NB (1999) Accepting the standardized precipitation index: a calculation algorithm. J Am Water Resour As 35:311–322

Hagman G (1984) Prevention better than cure: report on human and natural disasters in the third world. Swedish Red Cross, Stockholm

Halwatura D, McIntyre N, Lechner AM, Arnold S (2017) Capability of meteorological drought indices for detecting soil moisture droughts. J Hydrol Reg Stud 12:396–412

Hao Z, Singh VP (2015) Drought characterization from a multivariate perspective: a review. J Hydrol 527:668–678

Hao C, Zhang J, Yao F (2015) Combination of multi-sensor remote sensing data for drought monitoring over Southwest China. Int J Appl Earth Obs Geoinf 35(Part B):270–283

Harris I, Jones PD, Osborn TJ (2014) Updated high-resolution grids of monthly climatic observations-the CRU TS3.10 dataset. Int J Climatol 34(3):623–642

Hayes MJ, Svoboda MD, Wilhite DA, Vanyarkho OV (1999) Monitoring the 1996 drought using the standardized precipitation index. Bull Am Meteorol Soc 80(80):429–438

He Y, Lee E, Warner TA (2017) A time series of annual land use and land cover maps of China from 1982 to 2013 generated using AVHRR GIMMS NDVI3g data. Remote Sens Environ 199:201–217

Huang RH, Cai RS, Chen JL, Zhou LT (2006) Interdecadal variations of drought and flooding disasters in China and their association with the East Asian Climate System. Chin J Atmos Sci 30:730–743 (in Chinese)

Iguchi T, Kozu T, Meneghini R, Awaka J, Okamoto K (2000) Rain-profiling algorithm for the TRMM precipitation radar. J Appl Meteorol 39:2038–2052

Jackson TJ, Schmugge TJ (1991) Vegetation effects on the microwave emission of soils. Remote Sens Environ 36:203–212

Jiao W, Tian C, Chang Q, Novick KA, Wang L (2019a) A new multi-sensor integrated index for drought monitoring. Agric For Meteorol 268:74–85

Jiao W, Wang L, Novick KA, Chang Q (2019b) A new station-enabled multi-sensor integrated index for drought monitoring. J Hydrol 574: 169–180

Jiao W, Chang Q, Wang L (2019c) The sensitivity of satellite solar-induced chlorophyll fluorescence to meteorological drought. Earth's Future 7:558–573

Karnieli A, Agam N, Pinker RT, Anderson M, Imhoff ML, Gutman GG, Panov N, Goldberg A (2010) Use of NDVI and land surface temperature for drought assessment: merits and limitations. J Clim 23: 618–633

Kawanishi T, Sezai T, Ito Y, Imaoka K, Takeshima T, Ishido Y, Shibata A, Miura M, Inahata H, Spencer RW (2003) The advanced microwave scanning radiometer for the earth observing system (AMSR-E), NASDA's contribution to the EOS for global energy and water cycle studies. IEEE Trans Geosci Remote Sens 41(2):184–194

Keyantash JA, Dracup JA (2004) An aggregate drought index: assessing drought severity based on fluctuations in the hydrologic cycle and surface water storage. Water Resour Res 40(9)

Kimball BA (2016) Crop responses to elevated CO2and interactions with H2O, N, and temperature. Curr Opin Plant Biol 31:36–43

Kogan FN (1995) Droughts of the late 1980s in the United States as derived from NOAA polar-orbiting satellite data. Bull Am Meteorol Soc 76:655–668

Kogan FN (1997) Global drought watch from space. Bull Am Meteorol Soc 78(4):621–636

Liu Q, Zhang S, Zhang HR, Bai Y, Zhang JH (2020) Monitoring drought using composite drought indices based on remote sensing. Sci Total Environ 711:134585

Manderscheid R, Erbs M, Burkart S, Wittich K-P, Lopmeier F-J, Weigel H-J (2016) Effects of free-air carbon dioxide enrichment on sap flow and canopy microclimate of maize grown under different water supply. J Agron Crop Sci 202:255–268

McKee TB, Doesken NJ, Kleist J (1993) The relationship of drought frequency and duration to time scales. In: 8th Conference on Applied Climatology, Anaheim, pp 179–184

Meroni M, Rossini M, Guanter L, Alonso L, Rascher U, Colombo R, Moreno J (2009) Remote sensing of solar-induced chlorophyll fluorescence: review of methods and applications. Remote Sens Environ 113:2037–2051

Ministry of Natural Resources of the People's Republic of China. Current Land Use Classification (GB/T 21010–2011) [EB/OL]. (2011-07-01)

Mitchell SW, Remmel TK, Csillag F, Wulder MA (2008) Distance to second cluster as a measure of classification confidence. Remote Sens Environ 112:2615–2626

National Bureau of Statistics of China (NBSC) (2009) China Energy Statistical Yearbook. China Statistics Press, Beijing

National Bureau of Statistics of China (NBSC) (2011) China Energy Statistical Yearbook. China Statistics Press, Beijing

Njoku E, Jackson TJ, Lakshmi V, Chane T, Nghiem S (2003) Soil moisture retrieval from AMSR-E. IEEE T Geosci Remote 41:215–229

Orville H (1990) AMS statement on meteorological drought. Amer Meteorological Soc, Boston, pp 02108–03693

Owe M, Jeu RD, Holmes T (2008) Multisensor historical climatology of satellite-derived global land surface moisture. J Geophys Res Earth Surf 113(F1):196–199

Palmer WC (1965) Meteorological drought: US Department of Commerce. US Department of Commerce, Weather Bureau, Washington, DC

Parinussa RM, De Jeu RAM, Holmes TRH, Walker JP (2008) Comparison of microwave and infrared land surface temperature

products over the NAFE'06 research sites. IEEE Geosci Remote Sens Lett 5:783–787

Park S, Im J, Park S, Rhee J (2017) Drought monitoring using high resolution soil moisture through multi–sensor satellite data fusion over the Korean peninsula. Agric For Meteorol 237–238:257–269

Parkinson CL (2003) Aqua: an earth-observing satellite mission to examine water and other climate variables. IEEE Trans Geosci Remote Sens 41(2):173–183

Piao S, Ciais P, Huang Y, Shen Z, Peng S, Li JS, Zhou LP, Liu HY, Ma YC, Ding YH, Friedlingstein P, Liu CZ, Tan K, Yu YQ, Zhang TY, Fang JY (2010) The impacts of climate change on water resources and agriculture in China. Nature 467(7311):43–51

Pouya A, Hadigheh B, Ozgur K (2020) Comparison of three different bio-inspired algorithms to improve ability of neuro fuzzy approach in prediction of agricultural drought, based on three different indexes. Comput Electron Agric 170:105279

Powell MJD (1978) A fast algorithm for nonlinearly constrained optimization calculations. In: Numerical analysis. Springer, Berlin, Heidelberg, pp 144–157

Powell MJD (1983) Variable metric methods for constrained optimization mathematical programming the state of the art. Springer, pp 288–311

Quiring SM, Ganesh S (2010) Evaluating the utility of the vegetation condition index (VCI) for monitoring meteorological drought in Texas. Agric For Meteorol 150:330–339

Rhee J, Im J, Carbone GJ (2010) Monitoring agricultural drought for arid and humid regions using multi-sensor remote sensing data. Remote Sens Environ 114:2875–2887

Seiler R, Kogan F, Sullivan J (1998) AVHRR-based vegetation and temperature condition indices for drought detection in Argentina. Adv Space Res 21(3):481–484

Shahabfar A, Ghulam A, Eitzinger J (2012) Drought monitoring in Iran using the perpendicular drought indices. Int J Appl Earth Obs Geoinf 18:119–127

Shen ZX, Zhang Q, Singh VP, Sun P, Song CQ, Yu HQ (2019) Agricultural drought monitoring across Inner Mongolia, China: model development, spatiotemporal patterns and impacts. J Hydrol 571:793–804

Singh RP, Roy S, Kogan F (2003) Vegetation and temperature condition indices from NOAA AVHRR data for drought monitoring over India. Int J Remote Sens 24:4393–4402

Song LS, Li Y, Ren YH, Wu XC, Guo B, Tang XG, Shi W, Ma M, Han X, Zhao L (2019) Divergent vegetation responses to extreme spring and summer droughts in southwestern China. Agric For Meteorol 279:107703

Sun Y, Fu R, Dickinson R, Joiner J, Frankenberg C, Gu LH, Xia YL, Fernando N (2015) Drought onset mechanisms revealed by satellite solar-induced chlorophyll fluorescence: insights from two contrasting extreme events. J Geophys Res-Biogeo 120:2427–2440

Trenberth KE, Dai A, Rasmussen RM, Parsons DB (2003) The changing character of precipitation. B Am Meteorol Soc 84:1205–1217

Um MJ, Kim Y, Park D (2018) Evaluation and modification of the drought severity index (DSI) in East Asia. Remote Sens Environ 209:66–76

van Dijk AIJM, Beck HE, Crosbie RS, de Jeu RAM, Liu YY, Podger GM, Timbal B, Viney NR (2013) The millennium drought in Southeast Australia (2001–2009): natural and human causes and implications for water resources, ecosystems, economy, and society. Water Resour Res 49:1040–1057

Vicente-Serrano SM, Beguería S, Lopez-Moreno JI (2010) A multiscalar drought index sensitive to global warming: the standardized precipitation evapotranspiration index. J Clim 23:1696–1718

Wang A, Lettenmaier DP, Sheffield J (2011) Soil moisture drought in China, 1950–2006. J Clim 24:3257–3271

Wang L, D'Odorico P, Evans J, Eldridge D, McCabe M, Caylor K, King E (2012) Dryland ecohydrology and climate change: critical issues and technical advances. Hydrol Earth Syst Sci 16:2585–2603

Wang SH, Huang CP, Zhang LF, Lin Y, Cen Y, Wu T (2016) Monitoring and assessing the 2012 drought in the great plains: analyzing satellite-retrieved solar-induced chlorophyll fluorescence, drought indices, and gross primary production. Remote Sens 8(2):61

Wei W, Pang SF, Wang XF, Zhou L, Xie BB, Zhou JJ, Li CH (2020) Temperature vegetation precipitation dryness index (TVPDI)-based dryness-wetness monitoring in China. Remote Sens Environ 248: 111957. https://doi.org/10.1016/j.rse.2020.111957

Wells N, Goddard S, Hayes M J (2004) A Self-Calibrating Palmer drought severity index. J Clim 17:2335–2351

Wilhelmi OV, Wilhite DA (2002) Assessing vulnerability to agricultural drought: a Nebraska case study. Nat Hazards 25(1):37–58

Wu J, Zhou L, Liu M, Zhang J, Leng S, Diao C (2013) Establishing and assessing the integrated surface drought index (ISDI) for agricultural drought monitoring in mid-eastern China. Int J Appl Earth Obs Geoinf 23:397–410

Yuan X, Ma ZG, Pan M, Shi CX (2015) Microwave remote sensing of short–term droughts during crop growing seasons. Geophys Res Lett 42(11):4394–4401

Zhang AZ, Jia GS (2013) Monitoring meteorological drought in semiarid regions using multi-sensor microwave remote sensing data. Remote Sens Environ 134:12–23

Zhang X, Chen N, Li J, Chen Z, Niyogi D (2017) Multi-sensor integrated framework and index for agricultural drought monitoring. Environ Remote Sens 188:141–163

Zhou L, Zhang J, Wu J, Zhao L, Liu M, Lü A, Wu Z (2012) Comparison of remotely sensed and meteorological data-derived drought indices in mid-eastern China. Int J Remote Sens 33:1755–1779